

Comparison of the Head-Neck Kinematics of Different Active Human Body Models with Experimental Data

Oleksandr V. Martynenko, Isabell Wochner, Lennart V. Nölle, Eduardo H. Alfaro, Syn Schmitt,
Christian Mayer, Atul Mishra, Pronoy Ghosh, Ravi Kiran Chitteti, Jens Weber, María González-García,
Muriel Beaugonin, Stefanos Vlachoutsis

Abstract Up until now, various Active Human Body Models (AHBMs) have been developed using different anatomical references, validation data, modelling approaches and simulation software programs. Nevertheless, all these models should comply with the same validation requirements to deliver equivalent simulation results. This study focusses on the comparison of several AHBMs in different finite element software codes against the recently published experimental data for the head-neck kinematics. The main goal of such a comparison is the evaluation of the behaviour of different models when it comes to application in virtual testing procedures. Simulations were conducted based on a multi-dimensional simulation matrix varying two software codes, two muscle material models, two muscle control approaches and three existing AHBMs. Outcomes were compared to volunteer's head centre of gravity vertical displacement trajectories resulting in the CORA evaluation rating from marginal to fair (0,281 – 0,636).

Keywords Active Finite Element Human Body Model, Muscle Material Modelling, Extended Hill-type Muscle Material, Muscle Control Strategies, Neck muscles.

I. INTRODUCTION

In the past several years, Finite Element (FE) Active Human Body Models (AHBMs) have become a common tool for scientists and engineers working in the field of automotive safety systems development. At the same time, they continue to undergo development and validation processes. Thus far, a growing number of recent studies introduced AHBMs with the musculature and a controller operating on the full-body scale. The one worth mentioning are the SAFER AHBM [1], the THUMSv5 [2], the GHBMC [3], the THUMS TUC-VW AHBM [4] and the A-THUMS-D [5-6] models. As a result, AHBMs are more and more applied to the virtual development of advanced vehicle protection systems. Same as for the hardware testing, this process requires a comparable and harmonised outcome to be delivered by different models with the simulations run in various engineering software programs. Previous research has established the procedure to compare kinematics and results with various pedestrian human body models [7], but such works are rare for the AHBMs as of the authors' knowledge.

Different studies indicate the significance of appropriate control strategies for cervical muscles during low-speed events. The work [8] showed that both a control strategy mimicking the neural feedback of the vestibular system and a controller based on the muscle spindles' displacement feedback improved the head kinematics of the ViVA OpenHBM when compared to the passive model. Besides, the kinematic response of the SAFER AHBM was similarly improved by the use of closed loop controllers based on angular position and muscle length feedback in the study performed in [9]. The incorporation of the activation dynamics and reflex recruitment to GHBMC [10] and SAFER AHBM [11] FE models demonstrated improvement of vertebral kinematics and suggested the feasibility of such methods in predicting head-neck kinematics in low-severity impact scenarios.

The aim of this paper is to compare simulation results based on the multi-dimensional simulation matrix with the "Falling Heads" experimental data [12]. The simulation matrix dimensions consist of the two software codes

O. V. Martynenko (e-mail: oleksandr.martynenko@simtech.uni-stuttgart.de; tel: +49 711 685-68040) is a Senior Researcher, I. Wochner and L. V. Nölle are PhD students, E. H. Alfaro is a Master student and S. Schmitt is a Professor at the Institute for Modelling and Simulation of Biomechanical Systems, University of Stuttgart, Germany. Atul Mishra and Pronoy Ghosh are a Project Engineers and Ravi Kiran Chitteti is a Senior Program Manager in Human Body Modeling at Mercedes-Benz Research & Development, India. C. Mayer is a Program Coordinator at Mercedes-Benz AG, Germany. J. Weber is Research Engineer at Volkswagen Group Innovation, Volkswagen AG, Wolfsburg, Germany. M. González-García is a PhD Candidate at Ludwig Maximilian University, Munich, Germany and is employed at Volkswagen Group Innovation, Volkswagen AG, Wolfsburg, Germany. M. Beaugonin is a Biomechanics R&D Manager and S. Vlachoutsis is a Development Engineer at ESI Group, Rungis, France.

LS-DYNA and VPS; three AHBM models THUMS v5 [2], THUMS TUC-VW AHBM [4] and A-THUMS-D [5]; two Hill-type muscle material models [13-14] and two muscle control approaches of Lambda Control and Stretch Reflex Control.

II. METHODS

“Falling Heads” Experimental Data

We used the newly published “Falling Heads” experimental data [12] to investigate the head-neck complex’s response and passive properties as a basis for the comparison of AHBM models. The publication included 19 volunteers in total (10 female and 9 male). Height, weight, body mass index (BMI) and respective standard deviations for male subjects corresponding to FE AHBM models used are given in Table I.

During performed trials, volunteers were lying down on a horizontal table unrestrained in the supine position with the arms placed on the abdomen. The T1 vertebra was placed over the table’s edge, and the body maintained its relaxed position on the table under gravity. A specifically designed trapdoor supported the head. To account for the different anthropometries of the volunteers the table height and position in relation to the trapdoor were controlled to ensure that (1) the edge of the table is parallel and on the same height as the trapdoor, (2) the volunteer’s head is always placed in the same marked position on the top surface of the trapdoor. This head support was fixed in the space due to measuring equipment calibration reasons.

Participants were asked to completely relax their muscles, which was monitored by surface electromyography (EMG) of the *Sternocleidomastoideus* and the *Trapezius* muscles. The experiment started with a sudden release of the trapdoor when EMG signals were on background noise level for more than 0.5 s. After that, the head-neck complex was subjected to the gravitational load and moved downwards until the person contracted respective muscles, trying to compensate for the head fall movement.

Three markers attached to the head were tracked to identify its translational and rotational movements. Vertical displacement of Marker 2 (Fig. 1) corresponds to the head centre of gravity (COG) projection in the sagittal plane and will be utilized in the current study as a reference data. The authors believe that displacements data of only one marker could be considered accurate enough for the aims of the current study, considering that in [12]: 1) the THUMS v5 model results were validated against the quantities depending on the multiple markers signals and showed good correlation based on the L2 Loss Function error estimation; 2) A-THUMS-D and THUMS TUC-VW AHBM models will deliver results comparable to the THUMS v5 with the same initial and boundary conditions.

The choice of the experimental data was based on the fact that it deals with the head-neck complex, which is essential for occupant safety, and that it has a relatively simple setup that is easy to replicate. It allows to evaluate the contribution of existing model elements in the neck region (e.g. soft tissues material properties and contact definitions) and to test the performance of muscle controllers with different settings.

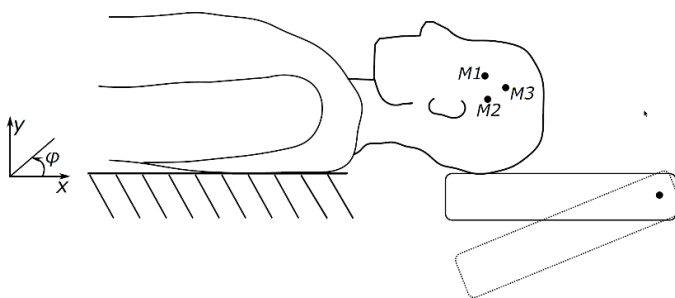


Fig. 1. Volunteer placement in a supine position as per experimental protocol for relaxed human behaviour study [12].

TABLE I

VOLUNTEER'S MEAN DATA VALUES [12]

Age [Years]	51.9 ± 20.7
Weight [kg]	72.0 ± 8.6
Height [m]	1.78 ± 0.03
BMI [kg/m ²]	22.6 ± 2.5

Muscle Material Models

Two different muscle materials, based on a macroscopic Hill-type formulation in two software codes, LS-DYNA [15] and Virtual Performance Solution (VPS) [16], were used in this work.

LS-DYNA

In LS-DYNA, the muscle materials used were *MAT_MUSCLE (*MAT_156) [13] and the user-defined Extended Hill-type material (EHTM) [14][17-18]. The first one has three simple elements in parallel: a contractile element (CE); a parallel elastic element (PEE); and a parallel damping element (PDE) (Fig. 2(a)). The second material consists of four elements: a CE and a PEE in series with a serial elastic element (SEE) and a serial damping element (SDE) (Fig. 2(b)). Hatze's activation dynamics function [19], which models the non-linear free calcium ion concentration and is dependent on the muscle length, was used to activate both materials. Additionally, the EHTM has an integrated controller that enables the use of the different control strategies [12][18] some of which were used in the current contribution and will be described in the following.

VPS

For VPS, the used 1D muscle materials are the Hill-type muscle material, corresponding to the structure presented in Fig. 2(a) and the extended Hill-type muscle material (EHTM), a tendon-muscle complex material following the structure shown in Fig. 2(b). The VPS EHTM material (type 241) is based on the implementation of EHTM made in LS-DYNA by [14]. As for VPS Hill-type material (type 240), the implementation architecture contains three sections. While the part of muscle type permits the definition of geometrical parameters, the EHTM material (type 241) definition manages all physical parameters and behaviours. The muscle activation characteristics are controlled by one of three activation models available for the VPS EHTM material (type 241). In addition to a time-dependent activation level by curve definition, which is already available for VPS material type 240, two dynamic activations can be selected: the Zajac dynamic activation model depending on the neural activation level, which is defined as a stimulation curve; and the Hatze dynamic activation model depending on the neural activation level and on length-dependent sensitivity of Ca^{2+} level change (see [14]). A comparison between the behaviour of both VPS muscle materials was carried out on concentric contraction load case experiments reported in [20] (see Appendix A).

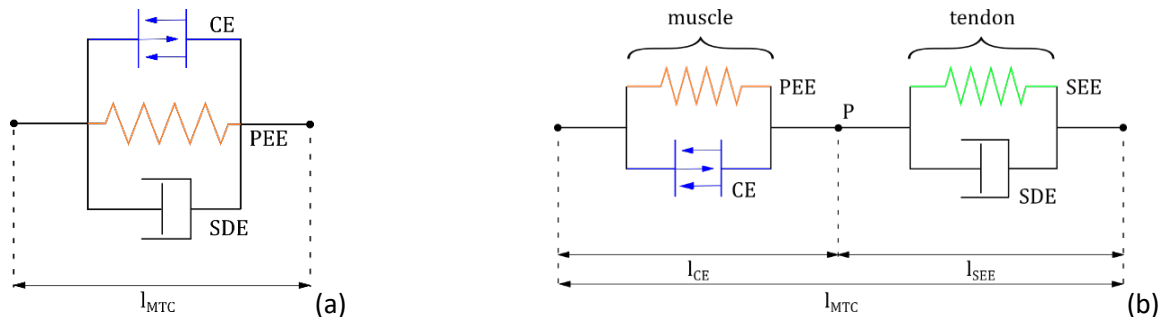


Fig. 2. Element structure of (a) the generic Hill-type muscle model existing in LS-DYNA (*MAT_156) and VPS (MAT_240) and (b) newly proposed Extended Hill-type muscle model [14].

For simplicity, the notation HTM (Hill-Type Muscle) will be used hereafter for the generic model existing in VPS (MAT_240) and LS-DYNA (*MAT_156), while the newly proposed MAT_241 in VPS and the *MAT_USER_DEFINED_MATERIAL_MODELS in LS-DYNA will be denoted as EHTM (Extended Hill-Type Muscle). Generic muscle parameters for both models are presented in Appendix B.

Muscle Elements Control Approaches

Two different closed-loop control strategies based on the muscle length are utilized in this study: (1) reflex controller; and (2) Lambda controller. The main difference between them is how the controlled variable is set before and monitored during the simulation. They have a different workflow depending on the software code used. These aspects are covered below.

LS-DYNA

The behaviour of the length-based feedback reflex controller integrated into EHTM can be defined by the user with four variables in the material card: the controller start time t_{contr} , the neural delay time τ , the reference length of the contractile element $l_{CE,ref}$ and the strain threshold ω [12][17][21]. The reflex controller is primed once the simulation time t has exceeded the sum of t_{contr} and τ . This allows for both the definition of a controller-

free model repositioning time at the start of the simulation through t_{contr} , as well as a representation of the biophysiological neural delay present in the human nervous system through τ . Once the reflex controller has been activated, the contractile element strain ε_{CE} is calculated using Equation (1):

$$\varepsilon_{CE} = \frac{l_{CE,delay} - l_{CE,ref}}{l_{CE,delay}} \quad (1)$$

with

$$l_{CE,delay} = l_{CE}(t - \tau). \quad (2)$$

If ε_{CE} surpasses the strain threshold ω , then a constant stimulation signal of $STIM=1$ is emitted by the reflex controller. This stimulation level is held as long as ε_{CE} is greater than zero. Only once $l_{CE,delay}$ is equal to or shorter in length than $l_{CE,ref}$ does the reflex controller cease to produce a muscle stimulation, and it will only be reactivated if $\varepsilon_{CE} > \omega$ at a later time step.

The threshold values $\omega = 0.02$ and $\omega = 0.05$ for the current study were selected based on the L2 Loss Function error estimation for the simulations with THUMSv5 performed for a range of threshold values (0.01-0.10) in [12]. This range is based on a preliminary study with the GHBMC model [10], where strain threshold sensitivity was evaluated using the CORA method and suggested a basis for the application of the reflex controller.

The second control option is a closed-loop controller based on the muscle length called the Lambda controller. It is meant to emulate the function of the muscle spindles, which sense the stretch of the muscle fibre and allow the human brain to regulate the muscle length to reach a desired state. The stimulation output of the Lambda controller u_λ is calculated as follows:

$$u_\lambda = \frac{k_p}{l_{CE,opt}} (l_{CE,delay} - \lambda) \quad (3)$$

where k_p is the controller proportional feedback gain (associated with muscle spindle signal), $l_{CE,opt}$ is the optimal contractile element fibre length, $l_{CE,delay}(t)$ is the delayed contractile element fibre length and λ is the desired contractile element length [6].

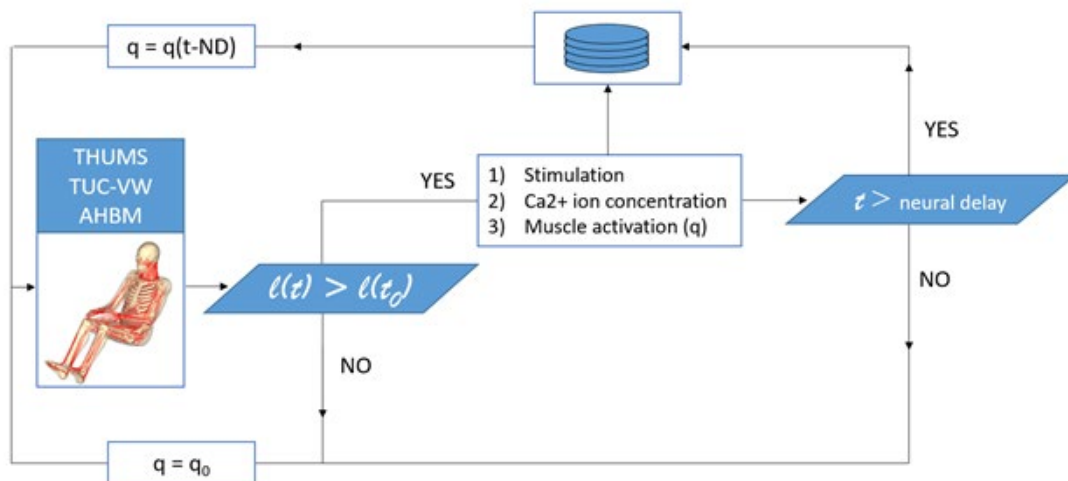


Fig. 3. Flowchart of the VPS-SimulationX coupling established for muscle feedback control in THUMS TUC-VW AHBM. q_0 is the muscle tone and ND – the neural delay.

VPS

The VPS-SimulationX coupling allows for the continuous exchange of data between the FE and one or more analytic model(s). To enable dynamic control of the muscle activation, the current exchange features of muscle-related quantities permit the transmission of parameters from the FE model, such as length, strain, strain rate and total force magnitude. On the other hand, the output variables of the muscle control are transferred to the FE model. This approach is used for the THUMS TUC-VW AHBM muscle control, particularly for the one based on

a closed-loop Lambda controller with the formulation presented in Equation (3) [4] (Fig. 3). The elongated muscles are activated to reach the target lengths given as input to the muscle algorithm. Furthermore, only in the case of the THUMS TUC-VW AHBM, an additional parameter has been integrated to account for the co-contraction of the antagonist muscles [22]. Specifically, a 5% co-contraction level is considered in this model. The developed dynamic control of the muscle activation is a function of the current muscle length and strain rate exported by VPS during the simulation. However, the muscle activation is not immediately exchanged to the AHBM, but rather is saved in a vector until the neural delay is reached [23-24]. In this study, the reflex control mentioned in Equation (1) was integrated into SimulationX, although in this case the strain variable considers the total muscle-tendon unit (MTU) length l_{MTU} instead of the contractile element length l_{CE} .

Active Finite Element Models Used in the Study

The three different FE AHBM used for the simulations are briefly described in the following paragraphs, complemented by the list of neck muscles for all models utilized in the study given in Appendix C.

THUMS v5

THUMS (Total Human Model for Safety) version 5.02.1 Academic, referred to hereafter as THUMS v5, was used in this study by the University of Stuttgart. THUMS v5 was jointly developed by Toyota Motor Corporation and Toyota Central R&D Labs. Inc [2] and aims to represent a 50th percentile male with a height of 175 cm and a weight of 74.0 kg, including 256 skeletal muscles comprising 808 parts with 1,726 elements [25]. Only 23 neck muscles, forming 90 parts with separate self-written controller code included into EHTM, were activated during simulations.

A-THUMS-D

A-THUMS-D is an AHBM developed for internal applications at Mercedes-Benz AG in LS-DYNA. The model represents a 50th percentile male with 175 cm height and 75.7 kg weight. The model has been implemented with 172 muscle groups (86 on each side of the body), represented by 878 beam elements (LS-DYNA ELFORM 3) [26]. The curvature of muscles was captured by using a routing approach with multiple beam elements in series connected at routing nodes. The *PART_AVERAGED keyword in LS-DYNA was used to maintain a common tensile force in all serially connected elements in each muscle strand.

Two different approaches to integrate a muscle controller dependent on the muscle material model (HTM or EHTM) are used in the model. For *MAT_MUSCLE, a Hybrid Equilibrium Point Controller (Hy-C) [6], coupled with activation dynamics proposed by [19], was incorporated as an external subroutine. The subroutine is coded in LS-DYNA common keywords. The associated *DEFINE_CURVE_FUNCTION keyword for each controlled muscle was set, and the curves were referred to in *MAT_MUSCLE. The neural delay was implemented using the *DELAY function. *MAT_MUSCLE governs the contraction dynamics of the muscle depending on the activity level computed by controller code, and axial stress is generated in a muscle based on the instantaneous activity level, muscle length and contraction velocity. For the EHTM, the built-in Lambda and Reflex controllers described above were used. A user manual on how to employ the two control methods can be found in [21].

THUMS TUC-VW AHBM

The AHBM used by Volkswagen in this study is the THUMS TUC-VW AHBM, a 50th percentile male (height: 175 cm, mass: 78.6 kg). This model is based on the THUMS TUC 2019 version realized in VPS code [16][27-28]. This is a passive HBM originally based on THUMS version 3.0 developed by Toyota Central R&D Labs., Inc. [29]. The initial upgrade towards an active HBM carried out at Volkswagen is described in detail in [4]. The AHBM has been further improved by performing necessary modifications concerning passive properties, with the aim of reducing the joint and overall HBM stiffness of the original THUMS v3 HBM, which is intended only for in-crash applications [4]. These improvements [30], also addressing the numerical robustness, are related to the soft tissue materials for passive muscle tissue and ligaments of the cervical vertebrae, according to available literature data [31-36]. The muscle action lines were modified from straight to curved paths to achieve biofidelic moment arms. In addition, muscle element fixations were attached to a larger area than just to a single node [37]. The complete model size is almost 240,000 nodes, including 654 1D-element muscle parts activated by 66 controllers.

Simulation Matrix of the Study

Simulations were conducted based on the multi-dimensional simulation matrix shown in Table II. The total number of simulations runs with and without the controller active for all FE AHBM and both muscle material models was 17. Six “relaxed” simulations with the controller deactivated were done to evaluate the passive properties of the models depending on the two different muscle materials. A reflex controller integrated into the EHTM [18] was applied with two different strain threshold values in the following six simulations. This parameter defines the maximum allowed elongation of the muscle, after which the feedback reflex controller based on the muscle length will be activated. Finally, five additional simulations with an active Lambda controller were performed. The value of the proportional gain k_p for the controller was derived from the equality condition to the reflex controller with a strain threshold of $\omega = 0.05$ following the methodology proposed by [12]. Simulations with the original THUMS v5 model using the standard LS-DYNA material *MAT_MUSCLE and the Lambda controller were not conducted as the model itself uses a posture control strategy based on joint angles monitoring and not the controller based on the muscle length [25].

TABLE II
SIMULATION MATRIX OF THE STUDY

Model	EHTM				HTM	
	No controller, “Relaxed”	Reflex controller, $\omega=0.02$	Reflex controller, $\omega=0.05$	Lambda controller, $K_p=15$	No controller, “Relaxed”	Lambda controller, $K_p=15$
THUMS v5	Yes	Yes	Yes	Yes	Yes	No
A-THUMS-D	Yes	Yes	Yes	Yes	Yes	Yes
THUMS TUC-VW AHBM	Yes	Yes	Yes	Yes	Yes	Yes

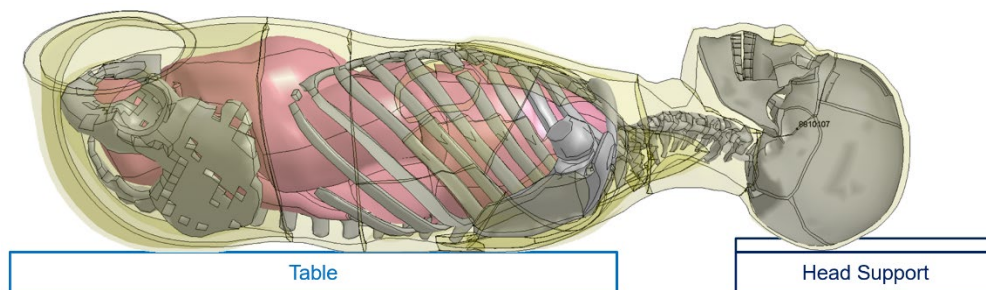


Fig. 4. Example of the FE AHBM in a supine position on the table and head trapdoor according to the experimental protocol initial conditions in [12].

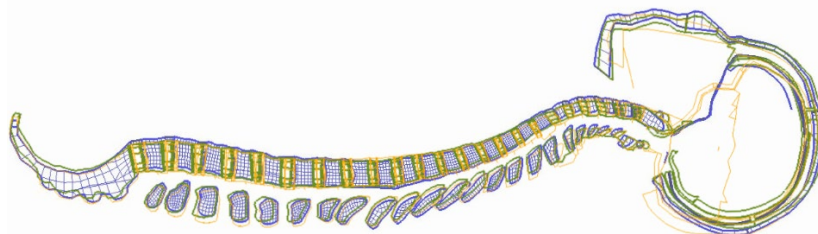


Fig. 5. Overlay of the relaxed models' relative vertebrae and skull position before simulations. THUMS v5 is shown in blue, A-THUMS-D in amber, and THUMS TUC-VW AHBM in green.

Boundary and Initial Conditions for Simulations

To replicate the experimental setup described in the Methods section above as closely as possible, T1 vertebra of each model was placed over the table's model edge. Trapdoors model was positioned on the same height parallel to the edge of the table. According to the setup (see Fig. 1), the weight of the arms is transferred to the table

through the elbows and shoulders, and the weight of the legs is applied directly to the table through skin contact. Moreover, bringing occupant models limbs into such a relaxed position would require large scale model modifications through the repositioning procedure, which is error prone. Therefore, to avoid the undesirable influence on the results, both upper and lower extremities were removed. Pelvis and sacrum were fixed in space to minimise the effects of the lower limbs' absence and to model their weight.

After initial positioning, simulations were done to settle the models under gravity on the table and head support (to bring them into the "relaxed" volunteer state, Fig. 4). The resulting models were used as the initial models for all simulations. They were considered identical to the initial positions of the volunteer test subjects during the experimental trials.

CORA Correlation Analysis

The correlation analysis software CORAplus version 4.0.4 was used to evaluate the simulation results for AHBM's against experimental data [38]. CORAplus provides validation metrics ranging from 0 (poor match) to 1 (perfect match) for the range of signals obtained from experimental and computational studies. The CORA global settings for the interval of evaluation, corridor and cross-correlation, same as the weighting factors, were kept default.

III. RESULTS

Evaluation of the initial and boundary conditions for the models is provided below. Vertical displacement of the head COG for all three AHBM's and simulated load cases is shown on separate figures and compared to the experimental data. Results are grouped based on the specific control approaches and muscle models for ease of reading and comparison.

Evaluation of Boundary and Initial Conditions Similarity between Models

To ensure similar initial positions, including internal vertebra and skull postures after relaxation, and to secure comparable simulation outcomes for all three FE AHBM's, an overlay of the model cross-sections in the median plane was created (Fig. 5). As seen, good correlation between positions was achieved. Furthermore, a lateral view of the three models is provided in Appendix D.

Vertical displacement trajectories

To assess the simulation results, vertical displacement trajectories for the head COG of all three models were compared based on the suggestions from the Methods section. Maximal vertical displacements for all models and all load cases are presented in Table III. For a clear graphical analysis, the 17 simulations are divided into three main categories per the muscle activation scheme: no controller activation (Fig. 6); active reflex controller (Fig. 7); and active Lambda controller (Fig. 8).

TABLE III
MAXIMAL VERTICAL DISPLACEMENTS FOR DIFFERENT LOAD CASES [M]

Model	EHTM				HTM	
	No controller, "Relaxed"	Reflex controller, $\omega=0.02$	Reflex controller, $\omega=0.05$	Lambda controller, $K_p=15$	No controller, "Relaxed"	Lambda controller, $K_p=15$
THUMS v5	-0.125	-0.095	-0.116	-0.125	-0.135	—
A-THUMS-D	-0.135	-0.078	-0.112	-0.095	-0.132	-0.093
THUMS TUC-VW AHBM	-0.126	-0.111	-0.125	-0.109	-0.119	-0.093

No Active Controller

Figure 6 shows that the head COG displacement trajectories of all three models follow the slope of the lower experimental trajectories until the point when some of the volunteers begin to activate their muscles (detected latency times between 0.18 and 0.087 s [12]). After this moment, simulation results start to fall below the volunteer trajectories which is explained by the model's properties and the fact that AHBM's have no controller

active (see Discussion section for more details). Corresponding CORA ratings for the simulations are in range [0.524 – 0.600] and can be found in the Table IV.

It is worth mentioning that for the initial 0.08 s all the models behave in a similar manner. After this point, they split into two groups based on the slope behaviour. The A-THUMS-D and the THUMSv5 using the HTM fall faster than the THUMS TUC-VW AHBM and the THUMSv5 with the EHTM material model. As for the difference between EHTM and HTM material models, the displacement trajectories follow the same pattern, but the EHTM implemented in THUMS v5 model makes its behaviour stiffer, while the opposite applies for THUMS TUC-VW AHBM and A-THUMS-D. It is also observed that the A-THUMS-D model shows higher vertical displacements in the relaxed state compared to both other models.

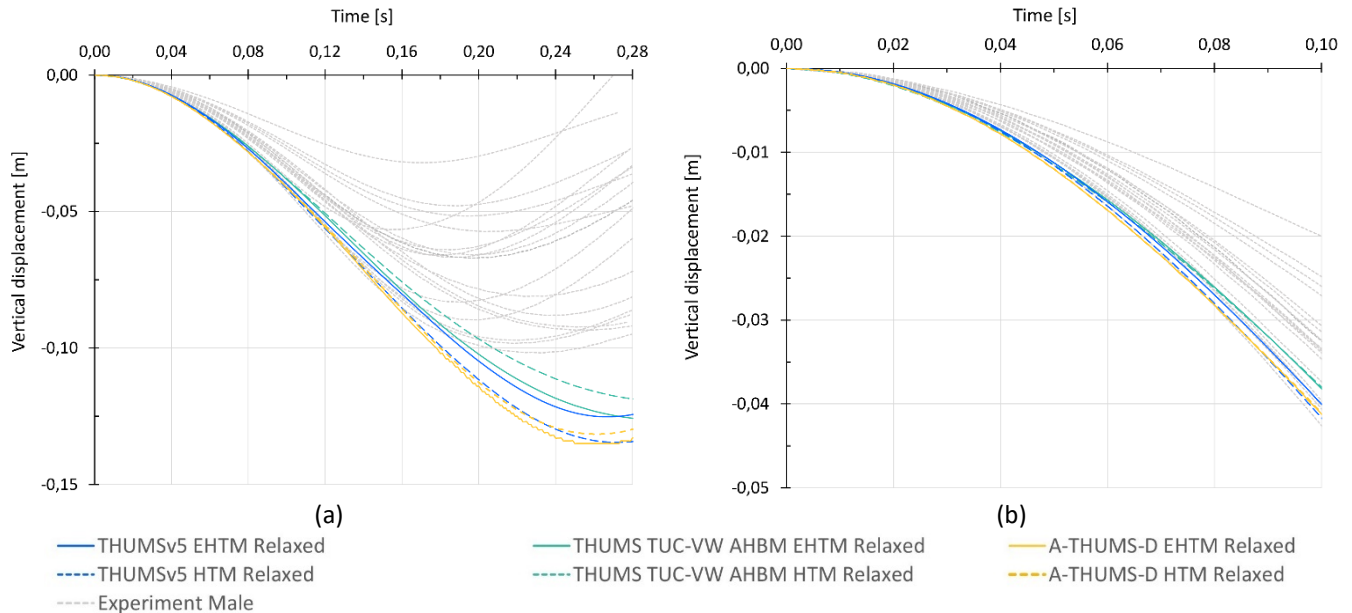


Fig. 6. Vertical displacement trajectories for the “Relaxed” models without muscle controller active. Time intervals on the horizontal axes correspond to the entire experiment lengths (a) and 0.100 s “Zoom in” (b).

Active Reflex Controller

The reflex muscle controller simulation results, with activation thresholds set to $\omega = 0.02$ and $\omega = 0.05$ and with the rest of the boundary and initial conditions remaining consistent, are displayed in Fig. 7. For all AHBM, the displacement trajectory with a lower reflex threshold lies above the trajectory with a higher one. In terms of maximum-minimum displacement, the envelope range is defined by the THUMS TUC-VW AHBM EHTM, the lower results boundary with $\omega=0.05$, and A-THUMS-D EHTM, the upper results boundary with $\omega=0.02$, respectively. Quantitative comparison with the CORA method is provided in the Table IV with the score being in range [0.349 – 0.656].

A-THUMS-D model shows the best correlation with the experimental results, being inside the experimental corridor with $\omega = 0.02$ (CORA rating 0.656) and slightly lower than the corridor with $\omega = 0.05$ (rating 0.424). THUMS v5 retains the slope of the experimental curves being in the lower boundary of the corridor for $\omega = 0.02$ (CORA rating 0.628) and below it for $\omega = 0.05$ (rating 0.352). THUMS TUC-VW AHBM results are falling below the corridor for both thresholds, which is partially explained by the difference in reflex controller code implementation. CORA rating is 0.374 for $\omega = 0.02$ and 0.349 for $\omega = 0.05$. This is addressed in the Discussion section.

Active Lambda Controller

As shown in Fig. 8, the HTM model produces less displacement compared to EHTM for two FE AHBM when applying the Lambda controller strategy. The THUMS v5 EHTM establishes the lower limit trajectory producing the maximum vertical displacement, with a value of -0.125 m (CORA rating 0.281) in contrast to A-THUMS-D HTM -0.095 m (CORA rating 0.636 for HTM and 0.598 for EHTM). THUMS TUC-VW AHBM lies between these values with both materials, having a maximum upper limit trajectory value of about -0.093 m. CORA ratings are 0.634 for HTM and 0.448 for EHTM, respectively. One interesting aspect is that the A-THUMS-D reaches the maximum

excursion about 0.030 s earlier than the THUMS TUC-VW AHBM. However, different maximum excursion times can also be observed for the volunteers, ranging from 0.160 s to 0.266 s.

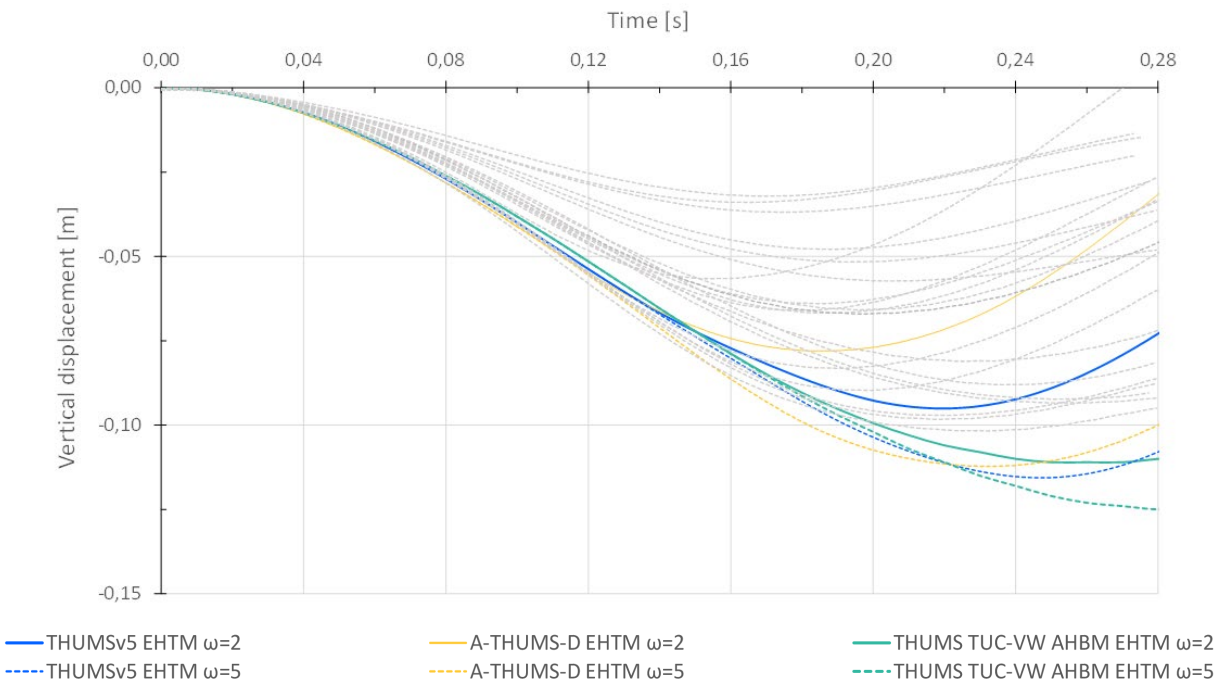


Fig. 7. Vertical displacement trajectories for the reflex muscle controller.

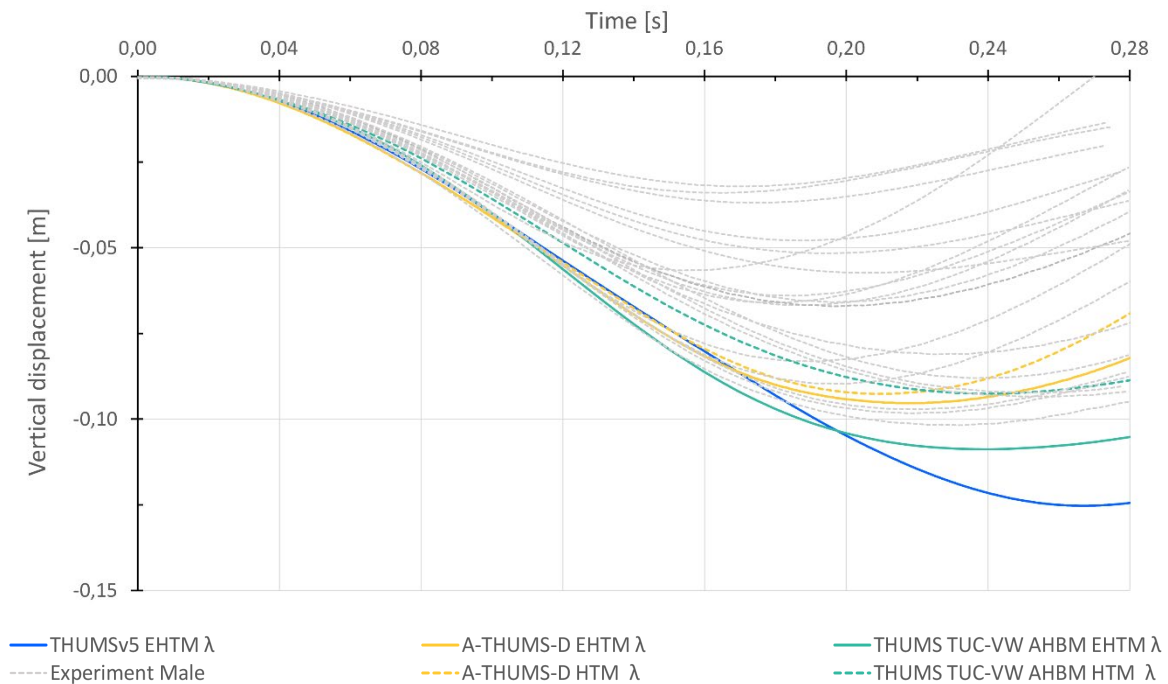


Fig. 8. Vertical displacement trajectories for the Lambda muscle controller.

CORA Quantitative Rating

For the simulations with the relaxed models, the evaluation interval of 0.0-0.8 s was used for the CORA rating, as the burst of the muscle response began after that time according to experimental EMG measurements [12]. For the rest of simulations, the whole interval of 0.0-0.280 s was considered. Results of the quantitative rating evaluation is presented in the Table IV and on the Fig. 9.

TABLE IV
CORA QUANTITATIVE RATING FOR DIFFERENT LOAD CASES

Model	EHTM				HTM	
	No controller, "Relaxed"	Reflex controller, $\omega=0.02$	Reflex controller, $\omega=0.05$	Lambda controller, $K_p=15$	No controller, "Relaxed"	Lambda controller, $K_p=15$
THUMS v5	0.600	0.628	0.352	0.281	0.524	–
A-THUMS-D	0.580	0.656	0.424	0.598	0.529	0.636
THUMS TUC-VW AHBM	0.588	0.374	0.349	0.448	0.596	0.634

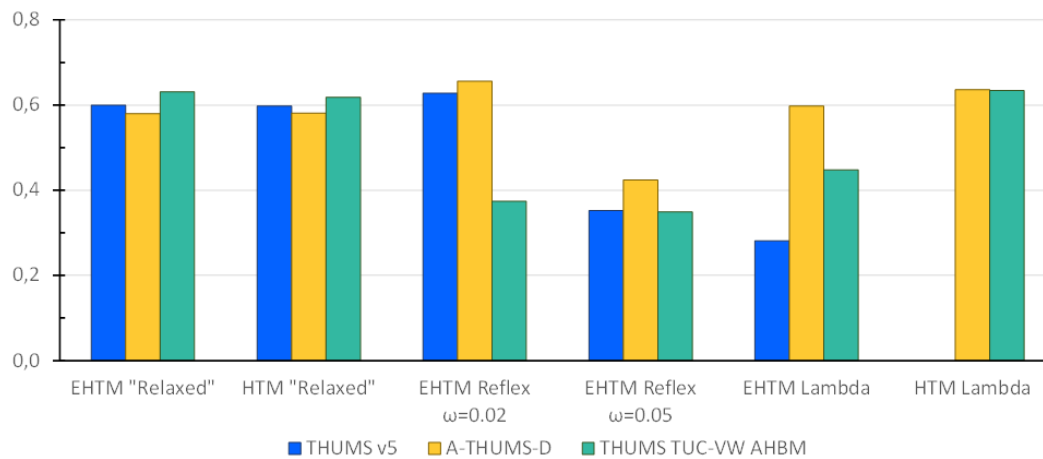


Fig. 9. CORA quantitative rating for different load cases.

IV. DISCUSSION

The current study found a difference in the simulations compared to the experimental volunteer's behaviour. One can imagine the main reason for such discrepancy being the material properties of the soft tissues composing the head-neck region. This issue could be addressed by additional validations and improvements of AHBM's passive properties. Such studies should take into account that mostly soft tissue material properties were obtained from cadaver subjects and modified according to specific procedures, which do not include reflexive experiments like the one presented in [39]. Therefore, more research seeking to identify relaxed volunteer behaviour is needed. Another reason lies in the muscle state during experiment, which should be considered. A certain level of muscle activation is always present in the living human body, even when relaxed, which was not taken into account by the control strategies used in this study. Consequently, standardization of the term "relaxed" regarding AHBM's is also required [3][40-41]. For the experiments used in this study the term "relaxed" means that the volunteers were asked to relax their muscles before the onset of the movement which was checked based on the level of background EMG activity [12]. An Additional example of relaxed volunteer experiments is given in [42]. Proposed leg flexion experiments could be added to a more comprehensive validation database for AHBM's.

A limitation of this study from the controller perspective is the absence of its omnidirectional application. However, previous studies have shown that muscle controllers proposed to be used do not depend on the model orientation in the global coordinate system, and therefore function adequately under any set of boundary conditions and in any direction. Lambda controller was implemented successfully for the lane change manoeuvre in [6], where simulation results were compared to the head COG excursion monitored in the sagittal plane (XOZ plane of the SAE coordinate system plane). The reflex mechanisms based on the muscle lengths feedback were successfully incorporated and tested against experimental impact data for GHBM [43] and VIVA OpenHBM [8] models. Relatively low CORA rating estimation of the vertical displacements in the Z direction of the SAE coordinate system for the mentioned studies showed that more efforts should be put into the investigation of muscle controller functioning for this direction. Accordingly, these shortcomings should be addressed in future

studies.

When considering the reflex control strategy (Fig. 7.), the maximal excursion is reached at different times for the three AHBM. This can be attributed to the difference in the EHTM Reflex controller implementation between LS-DYNA and VPS. For both THUMS v5 and A-THUMS-D, the strain calculation is based solely on the muscle fibre length l_{CE} and does not include the tendon length. The THUMS TUC-VW AHBM controller in VPS does not distinguish between muscle and tendon length and operates on the whole MTU-length l_{MTU} . Hence, the calculated muscle strain for the whole MTU will increase slower than the one in the CE alone, leading to a slightly delayed AHBM response and lower activation levels. This explains why THUMS TUC-VW AHBM reaches its maximal excursion later than the other two models while using the same controller parameters and reflex strategy. The same explanation applies for the lambda controller using the EHTM material. For this reason, the THUMS TUC-VW AHBM with the EHTM shows a later reaction than with the Hill type material modelling. Therefore, the study has motivated the aim to having access to the l_{CE} for the EHTM using coupling muscular control in VPS.

On the question of difference in the results for material models with Lambda controller strategy applied, this study found that AHBM with EHTM material show slower kinematic response compared to the one with HTM. This may be influenced by the difference in material elementary structure (see Fig. 2). Thus, having no tendon representation, HTM contracts faster compared to EHTM under the same activation. This should be taken into account when using the same controller parameters for both material models.

For the sake of comparison, the same controller gain Kp value was used for all the models considered in this study in accordance with the recommendation from [12] for THUMS v5. However, it is essential to highlight here, that controller parameters are model dependent and should be optimized accordingly for A-THUMS-D and THUMS TUC-VW AHBM. In such a way, higher CORA objective rating values could be achieved than those reported in Fig. 9. However, the authors believe that AHBM's response should be compared with the whole range of volunteer behaviour and not merely to the particular "average" behaviour.

V. CONCLUSIONS

This study used the "Falling Heads" experimental dataset as a benchmark to compare various AHBM in different FE software codes and to provide qualitative and quantitative conclusions that are valuable for researchers and simulation engineers. We evaluated different muscle materials and muscle control strategies via 17 simulations. Even though THUMS v5, A-THUMS-D and THUMS TUC-VW AHBM are derived from the same ancestor model, they should be treated as a "population", not as a "unique individual", when interpreting the results obtained. Therefore, they deliver comparable but not coinciding results in terms of head kinematics reported in the experiments. The reasons for the head displacement differences observed in simulations between models and in experiment are soft tissue material properties and controller's parameters.

VI. ACKNOWLEDGEMENTS



This work was supported by Deutsche Forschungsgemeinschaft (DFG, German Research Foundation) under Germany's Excellence Strategy - EXC 2075 - 390740016 (SimTech) and by the EU Horizon 2020 research and innovation program under grant agreement No. 768947 "OSCCAR".



This document reflects only the authors' views, the Innovation and Networks Executive Agency (INEA) is not responsible for any use that may be made of the information it contains.

VII. REFERENCES

- [1] Östth, J., Brolin, K., Bråse, D. (2015) A human body model with active muscles for simulation of pretensioned restraints in autonomous braking interventions. *Traffic Injury Prevention*, **16**(3): pp.304–313.
- [2] Iwamoto, M., Nakahira, Y. (2015) Development and Validation of the Total HUMAN Model for Safety (THUMS) Version 5 Containing Multiple 1D Muscles for Estimating Occupant Motions with Muscle Activation During Side Impacts. *Stapp Car Crash Journal*, **59**: pp.53–90.
- [3] Devane, K., Johnson, D., Gayzik, F.S. (2019) Validation of a simplified human body model in relaxed and braced conditions in low-speed frontal sled tests. *Traffic Injury Prevention*, **20**(8): pp.832–837.

- [4] Yigit, E. (2018) *Reaktives FE-Menschmodell im Insassenschutz*. AutoUni-Schriftenreihe 114, Springer Fachmedien Wiesbaden GmbH, Wiesbaden, Germany. DOI: https://doi.org/10.1007/978-3-658-21226_1-1.
- [5] Mishra, A., Ghosh, P., Chitteti, R. K., Mayer, C. (2020) Development of a Chinese 5th Percentile Female Active Human Body Model. *Proceedings of the IRCOBI Asia conference*, 2020, Beijing, China.
- [6] Martynenko, O. V., Neining, F. T., Schmitt, S. (2019) Development of a Hybrid Muscle Controller for an Active Finite Element Human Body Model in {LS-DYNA} Capable of Occupant Kinematics Prediction in Frontal and Lateral Maneuvers. *Proceedings of the 26th ESV Conference*, 2019, Eindhoven, Netherlands.
- [7] Klug, C., Feist, F., et al. (2017) Development of a procedure to compare kinematics of human body models for pedestrian simulations. *Proceedings of the IRCOBI conference*, 2017, Antwerp, Belgium.
- [8] Putra, I. P., Iraeus, J., et al. (2019) Comparison of control strategies for the cervical muscles of an average female head-neck finite element model. *Traffic Injury Prevention*, **20**(2): pp.116–S122.
- [9] Larsson, E., Iraeus, J., et al. (2019) Active Human Body Model Predictions Compared to Volunteer Response in Experiments with Braking, Lane Change, and Combined Manoeuvres. *Proceedings of the IRCOBI conference*, 2019, Florence, Italy.
- [10] Feller, L., Kleinbach, C., Fehr, J., Schmitt, S. (2016) Incorporating muscle activation dynamics into the Global Human Body Model. *Proceedings of the IRCOBI conference*, 2016, Malaga, Spain.
- [11] Ólafsdóttir, J. M., Östh, J., Brolin, K. (2019) Modelling reflex recruitment of neck muscles in a finite element human body model for simulating omnidirectional head kinematics *Proceedings of the IRCOBI conference*, 2019, Florence, Italy.
- [12] Wochner, I., Nölle, L. V., Martynenko, O. V., Schmitt, S. (2021) ‘Falling Heads’: investigating reflexive responses to head-neck perturbations. [Manuscript submitted].
- [13] Livermore Software Technology Corporation. (2016) *LS-DYNA Keyword User's Manual Volume II*, p.1479. LSTC, Livermore, California.
- [14] Kleinbach, C., Martynenko, O. V., et al. (2017) Implementation and validation of the extended Hill-type muscle model with robust routing capabilities in LS-DYNA for active human body models. *BioMedical Engineering Online*, **16**(1): pp.1–28. DOI: <https://doi.org/10.1186/s12938-017-0399-7>.
- [15] “LS-DYNA”, <http://www.lstc.com/products/ls-dyna> [cited March 2021].
- [16] “Virtual Performance Solution”, <https://www.esi-group.com/products/virtual-performance-solution>. [cited March 2021].
- [17] Martynenko, O. V., Kleinbach, C., et al. (2017) Advanced Hill-type Muscle model as User Defined Material in LS-DYNA with Routing Capability for Application in Active Human Body Models. *Proceedings of the IRCOBI conference*, 2017, Antwerp, Belgium.
- [18] Martynenko, O. V., Kempter, K., Kleinbach, C., Schmitt, S., Fehr, J. (2018) Integrated Physiologically Motivated Controller for the Open-Source Extended Hill-type Muscle Model in LS-DYNA. *Proceedings of the IRCOBI conference*, 2018, Athens, Greece.
- [19] Hatze, H. (1978) A general myocybernetic control model of skeletal muscle. *Biological cybernetics*, **28**(3): pp.143–157.
- [20] Günther, M., Schmitt, S., Wank, V. (2007) High-frequency oscillations as a consequence of neglected serial damping in Hill-type muscle models. *Biological Cybernetics*, **97**: pp.63–79. DOI <https://doi.org/10.1007/s00422-007-0160-6>.
- [21] Nölle, L. V., Lerge, P., Martynenko, O. V., Wochner, I. (2021) “Extended Hill-Type Muscle Material Model (EHTM) source code and manual”, <https://darus.uni-stuttgart.de/privateurl.xhtml?token=619c32c6-f157-4ca1-8bf0-147ed459628b>. [cited March 2021].
- [22] Günther, M., Ruder, H. (2003) Synthesis of two-dimensional human walking: a test of the λ -model. *Biological Cybernetics*, **89**: pp.89–106.
- [23] González-García, M., Weber, J., Kulavi, P. (2019) VPS-SimulationX Coupling for Active Human Body Modelling. *ESI Forum*, 2019, Berlin.
- [24] González-García, M., Weber, J., Peldschus, S. (2020) Numerical Study to Quantify the Potential Influence of Pre-Activated Muscles during the In Crash Phase. *8th International Symposium: Human Modeling and Simulation in Automotive Engineering*, 2020, Online.
- [25] *THUMS AM50 Academic Version 5.02.1 Manual*, p. 166. (2017) TOYOTA MOTOR CORPORATION and Toyota Central R&D Labs., Inc, Japan.

- [26] Mishra, A., Ghosh, P., *et al.* (2021) Development of the A-THUMS-D Active Human Body Model with Extended Hill-type Muscle Material Model and Stimulation Projection Strategy. [Manuscript submitted].
- [27] “TUC-Project – THUMS User Community”, <https://tuc-project.org/>. [cited March 2021].
- [28] “ESI Group: Empowering Industrial Players to Commit to Outcomes”, <https://www.esi-group.com>. [cited March 2021].
- [29] Iwamoto, M., Nakahira, Y., *et al.* (2007) Development of advanced human models in THUMS. *Proceedings of the 6th European LS-DYNA Users’ Conference*, 2007, Gothenburg, Sweden.
- [30] Davidson, J. *et al.* (2021) Validated and computationally robust active HBMs. Deliverable D3.2, OSCCAR Project; Grant Agreement No 768947; 2018
- [31] Nie, X., Cheng, J., Chen, W., Weerasooriya, T. (2010) Dynamic tensile response of porcine muscle. *Journal of Applied Mechanics*, **78**(2). DOI: <https://doi.org/10.1115/1.4002580>.
- [32] Song, B., Chen, W., Ge, Y., Weerasooriya, T. (2007) Dynamic and quasi-static compressive response of porcine muscle. *Journal of Biomechanics*, **40**(13): pp.2999–3005. DOI: <https://doi.org/10.1016/j.jbiomech.2007.02.001>.
- [33] Van Loocke, M., Lyons, C. G., Simms, C. K. (2008) Viscoelastic properties of passive skeletal muscle in compression: Stress-relaxation behaviour and constitutive modelling. *Journal of Biomechanics*, **41**(7): pp.1555–1566, DOI: <https://doi.org/10.1016/j.jbiomech.2008.02.007>.
- [34] Mattucci, S. (2011) Strain Rate Dependent Properties of Younger Human Cervical Spine Ligaments. *Journal of Kyoto Prefectural University of Medicine*, **10**: pp.216–226.
- [35] Mattucci, S., Moulton, J., Chandrasekhar, N., Cronin, D. (2012) Strain Rate Dependent Properties of Younger Human Cervical Spine Ligaments. *Journal of the Mechanical Behaviour of Biomedical Materials*, **10**, pp.216–226. DOI: <https://doi.org/10.1016/j.jmbbm.2012.02.004>.
- [36] Kulavi, P., Segura, R. D. (2016) Towards male specific material properties for cervical ligaments in finite element Human Body Models and its validation in functional spine units. *Proceedings of the IRCOBi conference*, 2016, Malaga, Spain.
- [37] Sugiyama, T., Weber, J., Sandoz, B., Bensler, H. P. (2018) Validation of a Reactive Finite Element Human Body Model under Moderate Lateral Loading. *7th International Symposium: Human Modeling and Simulation in Automotive Engineering*, 2018, Berlin.
- [38] Partnership for Dummy Technology and Biomechanics. (2017) *CORApplus Release 4.0.4 User's Manual*, p.76. PDB, Gaimersheim, Germany.
- [39] Van Ee, C.A., Chasse, A.L., Myers, B.S. (2000) Quantifying skeletal muscle properties in cadaveric test specimens: effects of mechanical loading, postmortem time, and freezer storage. *Journal of biomechanical engineering*, **122**(1): pp.9–14.
- [40] Meijer, R., Elrofai, H.B.H., Broos, W.J.C., van Hassel, E. (2013) Evaluation of an active multi-body human model for braking and frontal crash events. *23rd ESV Conference on Enhanced Safety of Vehicles*, 2013, Seoul, Korea.
- [41] Shelat, C., Ghosh, P., Chitteti, R., Mayer, C. (2016). “Relaxed” HBM – an Enabler to Pre-Crash Safety System Evaluation. *Proceedings of the IRCOBi conference*, 2016, Málaga, Spain.
- [42] Muehlbauer, J., González-García, M., Siebler, L., Schuck, S., Peldschus, S. (2020) Evaluation of Initial Volunteer Test Conditions in Locally Focused Validation Experiments for Active Human Body Model. *Proceedings of the IRCOBi conference*, 2020, Munich, Germany.
- [43] Correia, M. A., McLachlin, S. D., & Cronin, D. S. (2021). Vestibulocollic and Cervicocollic Muscle Reflexes in a Finite Element Neck Model During Multidirectional Impacts. *Annals of Biomedical Engineering*, 1-12.
- [44] Bayer, A., Schmitt, S., Günther, M., Haeufle, D. F. B. (2017) The influence of biophysical muscle properties on simulating fast human arm movements. *Computer methods in biomechanics and biomedical engineering*, **20**(8): pp.803–821.

VIII. APPENDIX A: EXPERIMENTAL VALIDATION OF THE HILL-TYPE MATERIAL MODELS

EHTM was implemented in both software codes before the study. The realization of LS-DYNA material is given in detail in [14, 18] and in VPS, which is described briefly below.

Figure A1 illustrates the improvement of simulated behaviour with VPS EHTM material (type 241) using the Hatze [19] activation dynamics in relation to the original VPS Hill-type material (type 240) on the example of a concentric contraction load case experiment with Piglet *calf* muscle reported in [20]. Figure A2 presents experimental data and similar simulation results with LS-DYNA. As already seen, for both VPS muscle materials the simulated maximum total force is identical. A comparable initial contraction velocity is simulated with VPS material type 240 and type 241, particularly for higher masses. Nevertheless, the VPS material type 240 cannot represent muscle velocity decrease in agreement with experimental results, in contrast to VPS EHTM material. In addition, a non-negligible effect of damping parameter in VPS material type 240 was noted. Tuning of this parameter could improve the obtained maximum velocity.

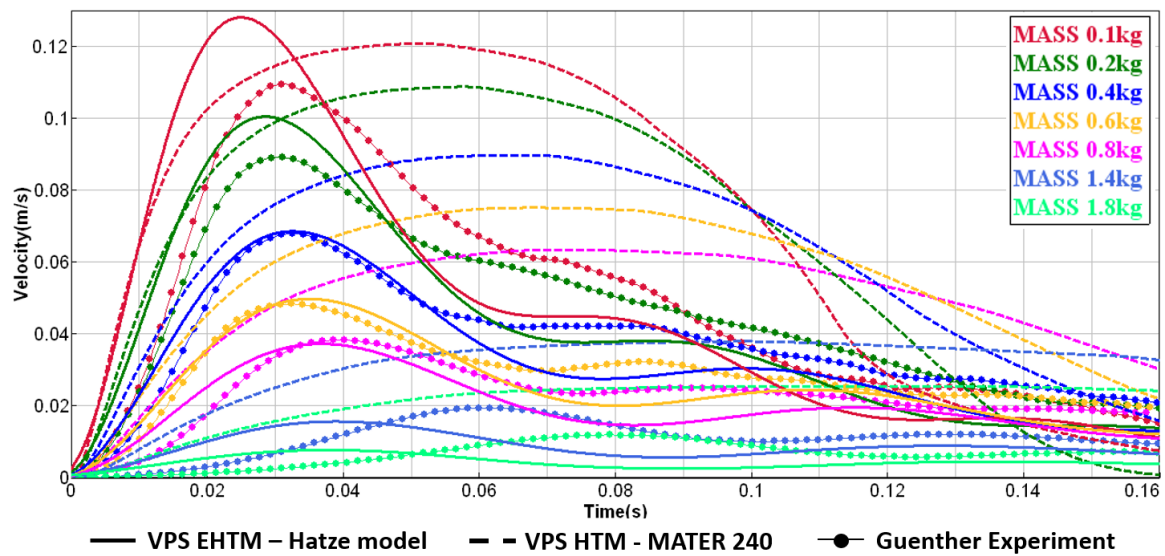


Fig. A1. Comparison of the concentric contraction velocities for Piglet *calf* muscle experiments (line with dots) and simulations involving suggested material types, MATER 240 (dashed line) and MATER 241 (EHTM, solid line), with Hatze activation dynamics in VPS.

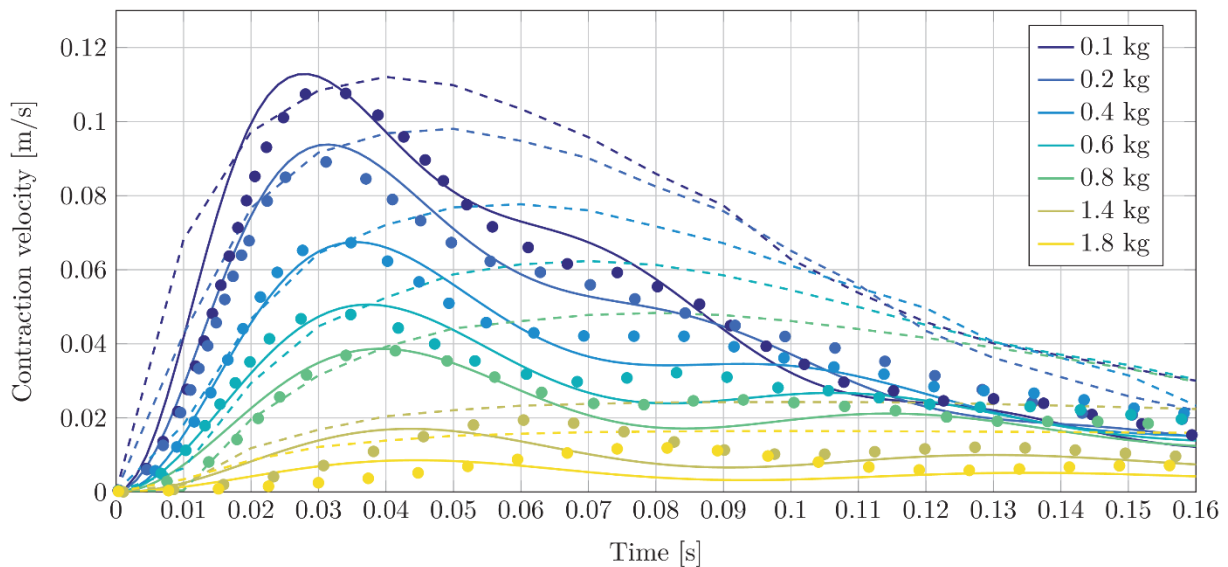


Fig. A2. Comparison of the concentric contraction velocities for Piglet *calf* muscle experiments (dots) and simulations involving suggested material types, *MAT_156 (dashed line) and EHTM (solid line), with Hatze activation dynamics in LS-DYNA [14].

IX. APPENDIX B: GENERIC MUSCLE PARAMETERS

The generic neck muscle parameters for EHTM material in all three models, taken from [44], are provided in Table B1. A detailed description of them in connection with the latest version of the EHTM FORTRAN code for LS-DYNA and the manual are available online [21]. Parameters for original HTM differ for various models and are available in the publications referenced in the section “Active Finite Element Models Used in the Study”.

TABLE B1
DETAILED DESCRIPTION OF GENERIC MUSCLE AND CONTROLLER PARAMETERS
USED FOR EHTM / 241 MATERIALS

Parameter	Units	Value in THUMS v5	Value in A-THUMS-D	Value in THUMS TUC-VW AHBM
$q0$	[-]	0.005	0.005	0.05
c	[mol/L]	1.3700E-4	1.3700E-4	-
eta	[L/mol]	52700.0	52700.0	-
k	[-]	2.9	2.9	-
m	[1/s]	11.3	11.3	-
$dWdes$	[-]	0.45	0.45	0.45
$nCEd$	[-]	1.5	1.5	1.5
$dWasc$	[-]	0.45	0.45	0.45
$nCEa$	[-]	3	3	3
$Arel0$	[-]	0.2	0.2	0.2
$Brel0$	[1/s]	2	2	2
$Secc$	[-]	2	2	2
$Fecc$	[-]	1.5	1.5	1.5
$LPEEO$	[-]	0.95	0.95	-
$nPEE$	[-]	2.5	2.5	2.5
$FPEE$	[-]	2	2	2
$dUSnll$	[-]	0.0425	0.0425	0.0425
$dUSl$	[-]	0.017	0.017	0.017
$Dsde$	[-]	0.3	0.3	0.3
$Rsde$	[-]	0.01	0.01	0.01
τ	[s]	0.025	0.025	0.025
k_p	[-]	15	15	15

X. APPENDIX C: MAIN NECK MUSCLE GROUPS ACTIVATED IN THE STUDY

TABLE C1

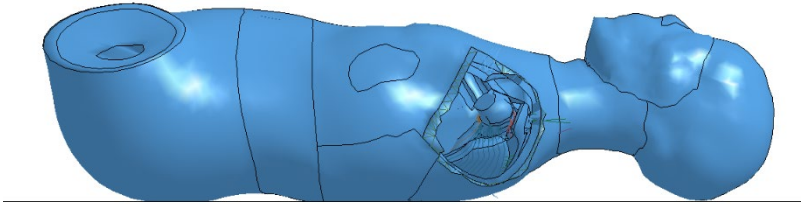

NECK MUSCLES REPRESENTED IN DIFFERENT MODELS

Muscle / Segment Name	THUMS v5	A-THUMS-D	THUMS TUC-VW AHBM
iliocostalis cervicis	Present	Present	Present
inferior oblique	Present	Present	Present
longissimus capitis	Present	Present	Present
longissimus cervicis	Present	Present	Present
longus capitis	Present	Present	Present
longus colli	Present	Present	Present
rectus capitis anterior	Present	Present	Present
rectus capitis lateralis	Present	Present	Present
rectus capitis posterior major	Present	Present	Present
rectus capitis posterior minor	Present	Absent	Present
scalenus anterior	Present	Present	Present
scalenus medius	Present	Present	Present
scalenus posterior	Present	Present	Present
semispinalis capitis	Present	Present	Present
semispinalis cervicis	Present	Present	Present
splenius capitis	Present	Present	Present
splenius cervicis	Present	Present	Present
sternocleidomastoid	Present	Present	Present
sternohyoideus	Present	Absent	Absent
superior oblique	Present	Present	Present
levator scapulae	Present	Present	Present
trapezius	Present	Present	Present

XI. APPENDIX D: COMPARISON OF THE AHBMs “RELAXED” POSITIONS

Position of all three HBMs in relation to the table and head support is shown in Table D1.

TABLE D1
POSITION OF THE AHBMS IN RELATION TO THE TABLE

Model	Position on the Side View
THUMS v5	
A-THUMS-D	
THUMS TUC-VW AHBM	